J Nanostruct 16(4): 4566-4576, Autumn 2026

RESEARCH PAPER

Nano-Encapsulated Date Palm Pollen Extract Protects HepG2 Cells Against Bisphenol A-Induced Oxidative Stress

Asaad H. Alzaidy *, Farah Razzaq Kbyeh, Mohamed Abdul Rida Yaseen

Department of Laboratory and Clinical Science, College of Pharmacy, University of Al Qadisiyah, Diwaniyah, Iraq

ARTICLE INFO

Article History:
Received 09 April 2026
Accepted 16 July 2026
Published 01 October 2026

Keywords:
Bisphenol A
Chitosan nanoparticles
Date palm pollen
Nano-encapsulation
Phoenix dactylifera

ABSTRACT

Bisphenol A (BPA) is a widespread endocrine-disrupting contaminant whose hepatotoxicity is driven, to a large extent, by oxidative stress. Date palm pollen (*Phoenix dactylifera* L., DPP) is a cheap and abundant source of phenolic antioxidants, but its practical use is limited by poor stability and low bioavailability. In the present work a phenolic-rich aqueous-ethanolic DPP extract was encapsulated in chitosan–tripolyphosphate nanoparticles by ionic gelation, and its ability to protect HepG2 cells from BPA-induced injury was compared with that of the free extract. The optimised nanoparticles were small and fairly uniform (mean diameter ≈ 196 nm; PDI ≈ 0.24), carried a positive surface charge (≈ +31 mV) and entrapped the extract efficiently (encapsulation efficiency ≈ 68%; loading capacity ≈ 19%). Successful loading was confirmed by FTIR, XRD and FESEM, which together indicated that the polyphenols were physically embedded within an essentially amorphous chitosan matrix of roughly spherical morphology. Exposure of HepG2 cells to BPA lowered viability and raised intracellular reactive oxygen species (ROS) and malondialdehyde, while depleting reduced glutathione and the activities of superoxide dismutase and catalase. Pre-treatment with the nano-encapsulated extract reversed these changes more strongly than the free extract at the same nominal dose, restoring antioxidant enzyme activity and returning ROS close to control values. The results suggest that chitosan-based nano-encapsulation markedly improves the cytoprotective performance of DPP polyphenols, and identify the nanoformulation as a promising candidate for limiting BPA-related hepatic oxidative damage.

How to cite this article
Alzaidy A., Kbyeh F., Yaseen M. Nano-Encapsulated Date Palm Pollen Extract Protects HepG2 Cells Against Bisphenol A-Induced Oxidative Stress. J Nanostruct, 2026; 16(4):4566-4576. DOI: 10.22052/JNS.2026.04.006

INTRODUCTION

Bisphenol A (BPA) is among the most heavily produced industrial chemicals worldwide, used mainly as a monomer in polycarbonate plastics and epoxy resins [1]. Because the bonds that link BPA to these polymers hydrolyse under heat and under acidic or alkaline conditions, the compound steadily migrates into food and beverages, and human exposure is now regarded as nearly universal [2]. The liver, as the principal site of xenobiotic metabolism, is a major target organ, and a number of studies have tied BPA to hepatic injury that is driven, at least partly, by the excessive generation of reactive oxygen

* *Corresponding Author Email: asaad.alzaidy@qu.edu.iq*

species (ROS) [3,4]. In hepatic cell models, even low and environmentally relevant concentrations of BPA disturb mitochondrial function, deplete the cellular antioxidant pool and promote lipid peroxidation [5,6]. The human hepatocellular carcinoma line HepG2 retains appreciable phase-II conjugation and some phase-I biotransformation activity and has therefore become a convenient *in vitro* platform for probing this kind of oxidative damage [7]. One practical way to limit such damage is to supply the cell with exogenous antioxidants; dietary polyphenols and flavonoids have repeatedly been shown to counteract oxidative insults, scavenging ROS and helping to restore endogenous antioxidant defences [8,9]. Among the less-exploited botanical sources of these compounds is date palm pollen (DPP), the fine powder produced by the male inflorescence of *Phoenix dactylifera* L. DPP is unusually rich in phenolic acids and flavonoids—rutin, catechin, gallic, ferulic, *p*-coumaric and syringic acids have all been reported—and crude DPP extracts display strong radical-scavenging and even anticancer activity towards HepG2 cells [10]. Date-palm extracts have likewise protected rodent liver against chemically induced oxidative damage [11,12]. Their translation is held back, however, by the poor aqueous solubility, chemical instability and rapid metabolism of polyphenols, which together give a low and erratic bioavailability [13,14]. Nano-encapsulation offers a route around these limitations: entrapping the bioactive load inside a polymeric matrix shields it from premature degradation, improves dispersibility and allows a slower, more sustained release [14,15]. Chitosan, a biodegradable and biocompatible cationic polysaccharide, is an attractive wall material because it self-assembles into nanoparticles by ionic gelation with tripolyphosphate (TPP) under mild aqueous conditions [15,16]. Although date palm pollen and related date-palm tissues have previously been encapsulated for antioxidant delivery—most recently in alginate beads that protected rat liver against BPA in vivo [17]—a chitosan–TPP nanoparticle carrier for DPP extract, evaluated in a BPA-challenged HepG2 model, has to our knowledge not been reported. The present study therefore set out to encapsulate a phenolic-rich DPP extract in chitosan–TPP nanoparticles, characterise the system by FTIR, XRD and FESEM, and test whether the nanoform protects HepG2 cells from BPA-induced oxidative stress more effectively than the free extract.

MATERIALS AND METHODS

Chemicals and reagents

Low-molecular-weight chitosan (degree of deacetylation ≈ 90%), sodium tripolyphosphate (TPP), bisphenol A (≥ 99%), 2,2-diphenyl-1-picrylhydrazyl (DPPH), 2′,7′-dichlorofluorescein diacetate (DCFH-DA), thiobarbituric acid, reduced glutathione, 5,5′-dithiobis-(2-nitrobenzoic acid) (DTNB), 3-(4,5-dimethylthiazol-2-yl)-2,5-diphenyltetrazolium bromide (MTT) and the Folin–Ciocalteu reagent were purchased from Sigma-Aldrich (St. Louis, MO, USA). Dulbecco's modified Eagle's medium (DMEM), fetal bovine serum (FBS), penicillin–streptomycin and trypsin–EDTA were obtained from Gibco (Thermo Fisher Scientific, USA). The remaining chemicals were of analytical grade and used as received, and deionised water was used throughout.

Plant material and preparation of the extract

Date palm pollen was collected from male *P. dactylifera* trees during the local pollination season, cleaned of debris and dried in the shade. The dried pollen was milled to a fine powder. A 50 g portion was extracted with 70% (v/v) aqueous ethanol at a solid-to-solvent ratio of 1:10 (w/v) under magnetic stirring for 24 h at room temperature. The mixture was centrifuged (4000 × g, 15 min) and the supernatant filtered through Whatman No. 1 paper. The filtrate was concentrated under reduced pressure at 40 °C, freeze-dried, and the resulting extract stored at −20 °C until use. An aqueous-ethanolic medium was chosen because DPP polyphenols are reasonably polar and to keep the protocol food-compatible [10].

Total phenolic and flavonoid content and phenolic profiling

The total phenolic content (TPC) was determined by the Folin-Ciocalteu technique [18] and reported in mg gallic acid equivalents per gram of extract (mg GAE/g). Total flavonoid concentration (TFC) was evaluated by aluminium-chloride colorimetric test and expressed as mg quercetin equivalents per gram (mg QE/g). Individual phenolic compounds were isolated and quantified by reversed-phase HPLC against authentic standards, under circumstances reported recently for palm pollen

extracts [10].

DPPH radical-scavenging activity

The free extract showed radical scavenging activity on the stable DPPH radical [19]. Briefly, aliquots of material at escalating concentrations were combined with a methanolic DPPH solution and maintained in the dark for 30 min. The absorbance was read at 517 nm. The inhibition % was plotted against concentration and the IC50 derived by interpolation, ascorbic acid was used as positive control.

Preparation of DPP-loaded chitosan nanoparticles

Nanoparticles were prepared by ionic gelation of chitosan with TPP, largely as reported by Calvo et al. [16] with slight modifications. Chitosan was dissolved in 1% (v/v) acetic acid to a 2 mg/mL solution, pH adjusted to around 4.7 and the solution filtered. A certain amount of freeze-dried DPP extract was added to the chitosan solution and mixed for 30 min to enable the polyphenols to bind with the polymer. TPP (1 mg/mL) was then added dropwise under continuous stirring (≈ 800 rpm) at room temperature, maintaining the mass

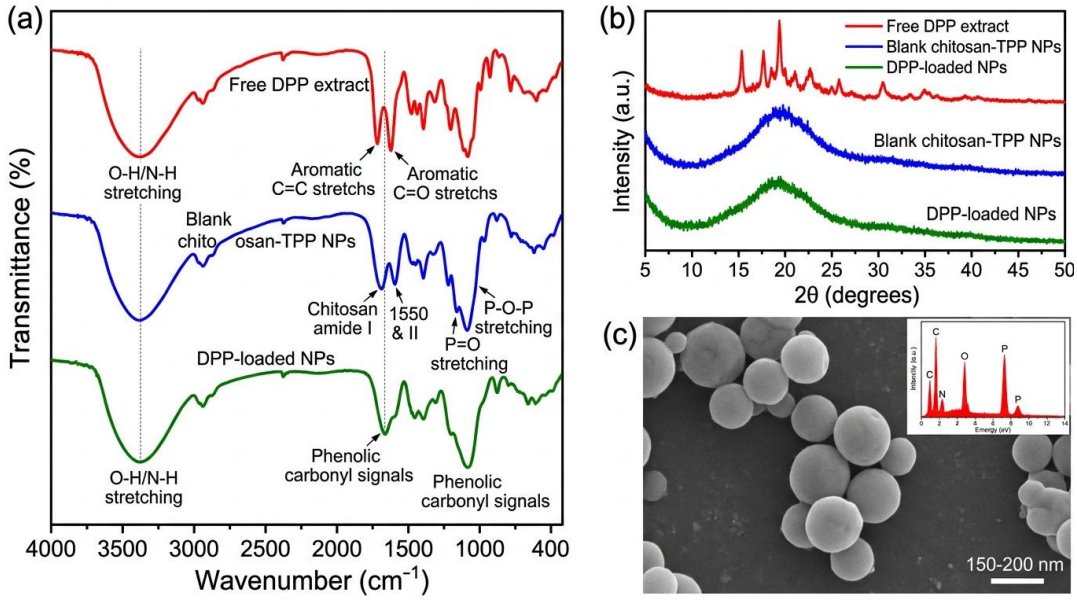

Fig. 1. Nano-characterisation of the date palm pollen extract and chitosan nanoparticles: (a) FTIR spectra of the free DPP extract, blank chitosan–TPP nanoparticles and DPP-loaded nanoparticles; (b) XRD patterns of the free DPP extract, blank chitosan–TPP nanoparticles and DPP-loaded nanoparticles; (c) representative FESEM micrograph of the DPP-loaded nanoparticles, with the corresponding EDX spectrum (inset) confirming the C, N, O and P signature of the cross-linked carrier.

Table 1. Total phenolic and flavonoid content, major HPLC-identified phenolic compounds, and DPPH radical-scavenging activity (IC_{50}) of the date palm pollen extract.

Parameter	Value (mean ± SD)
Total phenolic content (mg GAE/g)	92.4 ± 3.1
Total flavonoid content (mg QE/g)	38.2 ± 2.0
DPPH IC_{50} (µg/mL)	110 ± 6
Gallic acid (mg/g)	8.6 ± 0.4
Catechin (mg/g)	6.9 ± 0.3
Rutin (mg/g)	5.2 ± 0.3
p-Coumaric acid (mg/g)	4.1 ± 0.2
Ferulic acid (mg/g)	3.7 ± 0.2
Syringic acid (mg/g)	2.8 ± 0.2

ratio of chitosan to TPP close to 4:1. The resulting opalescent suspension was agitated for a further 40 min and then recovered by centrifugation (12,000 ×g, 30min, 4°C), rinsed with deionised water and freeze-dried with mannitol as cryoprotectant. At the same time, blank (unloaded) nanoparticles were obtained by removing the extract. The chitosan/extract ratios were varied from 1:0.25 to 1:1 and the best formulation in terms of particle size and encapsulation efficiency was selected [20].

Encapsulation efficiency and loading capacity

Encapsulation efficiency (EE) and loading capacity (LC) were determined indirectly. After centrifugation, the phenolics remaining in the supernatant were quantified by the Folin method and taken as the non-entrapped fraction. EE and LC were then calculated as:

EE (%) = [(total phenolics − free phenolics) / total phenolics] × 100

LC (%) = [(total phenolics − free phenolics) / weight of nanoparticles] × 100

All measurements were carried out in triplicate.

Physicochemical characterisation

Hydrodynamic diameter, polydispersity index (PDI) and zeta potential of the suspensions were measured at 25 °C by dynamic light scattering. Chemical interactions between the extract and the carrier were probed by Fourier-transform infrared (FTIR) spectroscopy over 4000–400 cm^{-1} using KBr discs. The crystalline or amorphous character of the powders was examined by X-ray diffraction (XRD) with Cu-Kα radiation over a 2θ range of 5–50°. Surface morphology was inspected by field-emission scanning electron microscopy (FESEM) after gold sputter-coating, and the elemental composition was checked with the coupled EDX detector. The FTIR spectra, XRD patterns and FESEM micrographs of the extract, the blank nanoparticles and the loaded nanoparticles are compiled in Fig. 1.

In vitro release

Release of phenolics from the nanoparticles was followed in phosphate-buffered saline (pH 7.4) and, separately, in acetate buffer (pH 5.5) at 37 °C under gentle shaking, using the dialysis-bag method. At preset intervals an aliquot of the receptor medium was withdrawn, replaced with fresh buffer, and its phenolic content measured. The cumulative release was plotted against time (Fig. 2).

Cell culture

HepG2 cells were maintained in DMEM supplemented with 10% FBS and 1% penicillin–streptomycin at 37 °C in a humidified atmosphere of 5% CO_2. Cells in the exponential growth phase were used for all experiments, and the medium was renewed every two days.

Cell viability and selection of the BPA challenge

Cytotoxicity was evaluated by the MTT assay [21]. Cells were seeded in 96-well plates (≈ 1 × 10^4 cells/well), allowed to attach overnight and treated for 24 h. To map the intrinsic safety of the carrier and of the extract, cells were exposed to a range of concentrations of free DPP extract, blank nanoparticles and loaded nanoparticles. In a separate set of plates, cells were treated with increasing concentrations of BPA to identify a dose that lowered viability to roughly 60–70% of control; this sub-lethal concentration was then used as the oxidative-stress challenge in the protection experiments. After treatment, MTT solution was added, the formazan crystals were dissolved in DMSO and the absorbance read at

Table 2. Physicochemical characteristics of the optimised DPP-loaded chitosan–TPP nanoparticles (mean particle size, polydispersity index, zeta potential, encapsulation efficiency and loading capacity).

Parameter	Value (mean ± SD)
Mean hydrodynamic diameter (nm)	196 ± 8
Polydispersity index (PDI)	0.24 ± 0.02
Zeta potential (mV)	+31 ± 2
Encapsulation efficiency (%)	68 ± 3
Loading capacity (%)	19 ± 1

570 nm. Viability was expressed as a percentage of the untreated control.

Experimental design for cytoprotection

For the protection study the cells were assigned to five groups: (i) untreated control; (ii) BPA alone (challenge dose); (iii) BPA + free DPP extract; (iv) BPA + loaded nanoparticles; and (v) loaded nanoparticles alone. In the protection groups the cells were pre-incubated with the test material for 4 h before BPA was added, and the co-incubation continued for 24 h. The non-cytotoxic dose identified by MTT was used for both the free and the encapsulated extract, so that the two forms could be compared at an equal nominal polyphenol dose (the amount of nanoparticles being scaled by the encapsulation efficiency so that the delivered polyphenol content, expressed as gallic acid equivalents, was matched between the two forms).

Intracellular ROS, lipid peroxidation, GSH and antioxidant enzymes

Intracellular ROS were quantified with the redox-sensitive probe DCFH-DA [22]. After treatment the cells were loaded with the probe, washed, and the fluorescence of the oxidised product measured (excitation ≈ 485 nm, emission ≈ 528 nm); results were normalised to the control. Lipid peroxidation was estimated from the malondialdehyde (MDA) content by the thiobarbituric-acid reactive substances method [23]. Reduced glutathione (GSH) was assayed with Ellman's reagent (DTNB) at 412 nm [24]. Superoxide dismutase (SOD) activity was measured by the pyrogallol-autoxidation method [25], and catalase (CAT) activity from the decomposition of hydrogen peroxide monitored at 240 nm [26]. Enzyme activities were normalised to the protein content of each lysate.

Statistical analysis

Every experiment was repeated at least three times and the data are given as mean ± standard deviation. Group means were compared by one-way ANOVA followed by Tukey's post-hoc test, taking $p < 0.05$ as significant. Analyses were carried out in standard statistical software.

RESULTS AND DISCUSSION

Phytochemical content and antioxidant activity of the extract

The freeze-dried DPP extract was a brownish, hygroscopic powder obtained in a yield of about 14% on a dry-weight basis. Its total phenolic

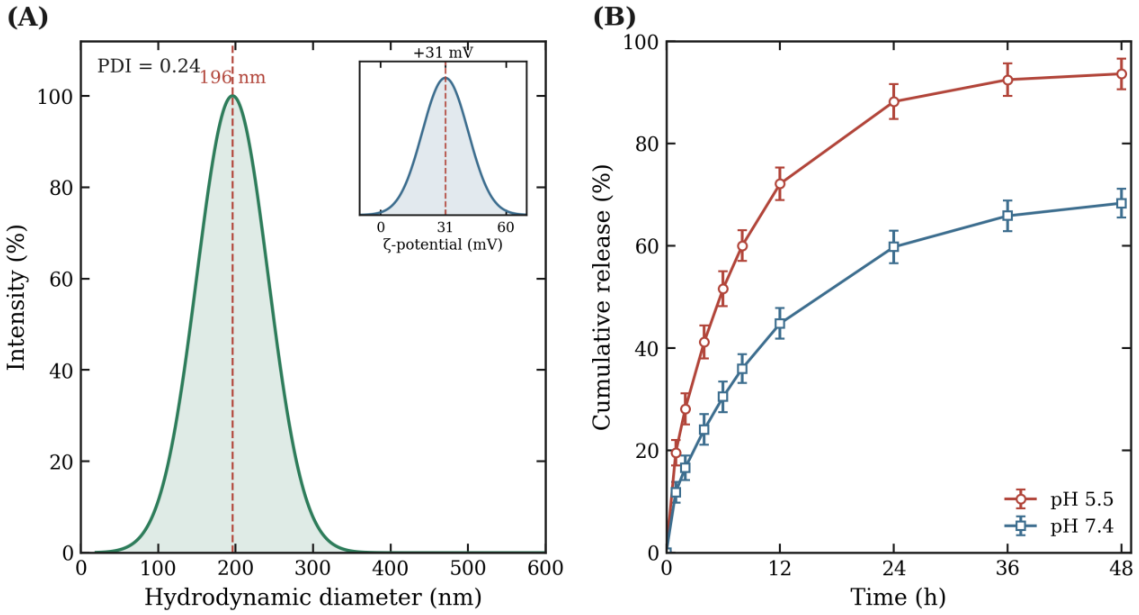

Fig. 2. Particle size distribution and zeta potential of the optimised DPP-loaded chitosan nanoparticles (a) and the in vitro cumulative release of phenolics at pH 5.5 and pH 7.4 over time (b).

content came to roughly 92 mg GAE/g and the flavonoid content to around 38 mg QE/g, values that sit comfortably within the range reported for palm pollen and other date-palm organs [10,27]. HPLC resolved a mixture dominated by gallic acid, catechin, *p*-coumaric, ferulic and syringic acids, together with the flavonoid glycoside rutin a fingerprint that matches closely the one Habib and co-workers described for palm fruit pollen [10]. In the DPPH assay the free extract scavenged the radical in a concentration-dependent manner, with an IC_{50} near 110 µg/mL. While this is weaker than ascorbic acid, it confirms a respectable antioxidant capacity that can plausibly be traced to the phenolic hydroxyl groups, which donate hydrogen atoms and stabilise the resulting radicals [9,12]. The detailed composition and the antioxidant indices are summarised in Table 1.

Encapsulation and physicochemical characterisation

Loading the extract into chitosan–TPP nanoparticles proved straightforward and reproducible. Across the ratios tested, the formulation prepared at a chitosan-to-extract ratio of about 1:0.5 gave the most favourable properties and was selected for the biological work. The chosen nanoparticles had a mean hydrodynamic diameter of approximately 196 nm with a PDI of about 0.24, pointing to a reasonably narrow size distribution, and a zeta potential of roughly +31 mV; the positive value arises from the protonated amino groups of chitosan that were not consumed in cross-linking. A surface charge of this magnitude is generally taken as a sign of good colloidal stability, since the particles repel one another and resist aggregation [16,20]. Encapsulation efficiency reached about 68% and loading capacity about 19%. These figures are a little higher than several comparable phenolic-loaded chitosan systems—for example, the grape-extract nanoparticles of Soleymanfallah et al., which showed a size and zeta potential of 177 nm and +33 mV at a similar ratio [20]—and the difference probably reflects the particular phenolic makeup of DPP and the affinity of its carboxyl- and hydroxyl-bearing acids for the chitosan backbone. Particle size, PDI, zeta potential, EE and LC are collected in Table 2.

FTIR spectra (Fig. 1) confirmed effective entrapment. The free extract shows a wide O–H/N–H band at around 3400 cm^{-1} and aromatic C=C and C=O stretches in the region of 1600–1700 cm^{-1} which are typical of phenolic acids. The typical chitosan amide bands and the vibrations

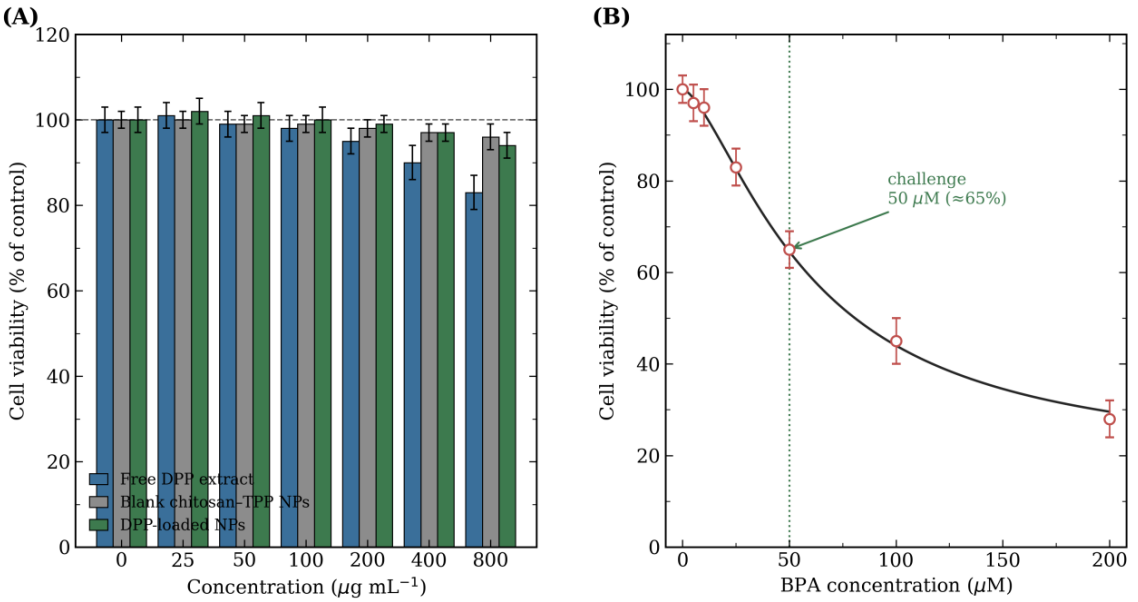

Fig. 3. a) Effect of the free DPP extract, blank chitosan–TPP nanoparticles and DPP-loaded nanoparticles on HepG2 viability (MTT assay) over the concentration range tested; (b) dose–response of HepG2 cells to bisphenol A, used to select the sub-lethal challenge concentration (50 µM, ≈ 65% of control viability). Data are mean ± SD (n ≥ 3).

of P=O and P-O-P of cross-linked TPP were clearly observed in the blank nanoparticles suggesting that ionic gelation had taken place. The extract loading caused a slight shift and broadening of the amine band of chitosan and the attenuation, but not the abolition, of the phenolic carbonyl signals, a pattern typically interpreted as physical entrapment and hydrogen-bonding between the polyphenols and the polymer, without the formation of major new covalent bonds [20]. This interpretation was supported by XRD (Fig. 1). The loaded nanoparticles were mainly amorphous, with the broad halo of chitosan replacing any sharp crystalline reflections. This is consistent with the extract being molecularly disseminated throughout the matrix, instead of a discrete crystalline phase. FESEM imaging (Fig. 1) revealed roughly spherical to subspherical particles with fairly smooth surfaces and only mild clustering. The sizes observed in the micrographs were broadly consistent with (though slightly smaller than) the hydrodynamic diameter from DLS, the difference being the familiar one between dried and hydrated states. The expected C, N, O and P signature of the cross-linked carrier was confirmed by EDX.

Fig. 2 shows a biphasic release profile. A rapid release over the first few hours, attributed to phenolics adsorbed at or near the surface, was followed by a slower continuous release driven by diffusion through and gradual relaxing of the chitosan network. The release at pH 5.5 was faster than at pH 7.4, which is consistent with the higher swelling of chitosan in moderately acidic conditions. This type of regulated protracted administration is precisely the advantage that one expects to obtain from nano-encapsulation, and elsewhere it has been connected to greater retention of the antioxidant activity and enhanced cellular availability of the payload [13,14,28].

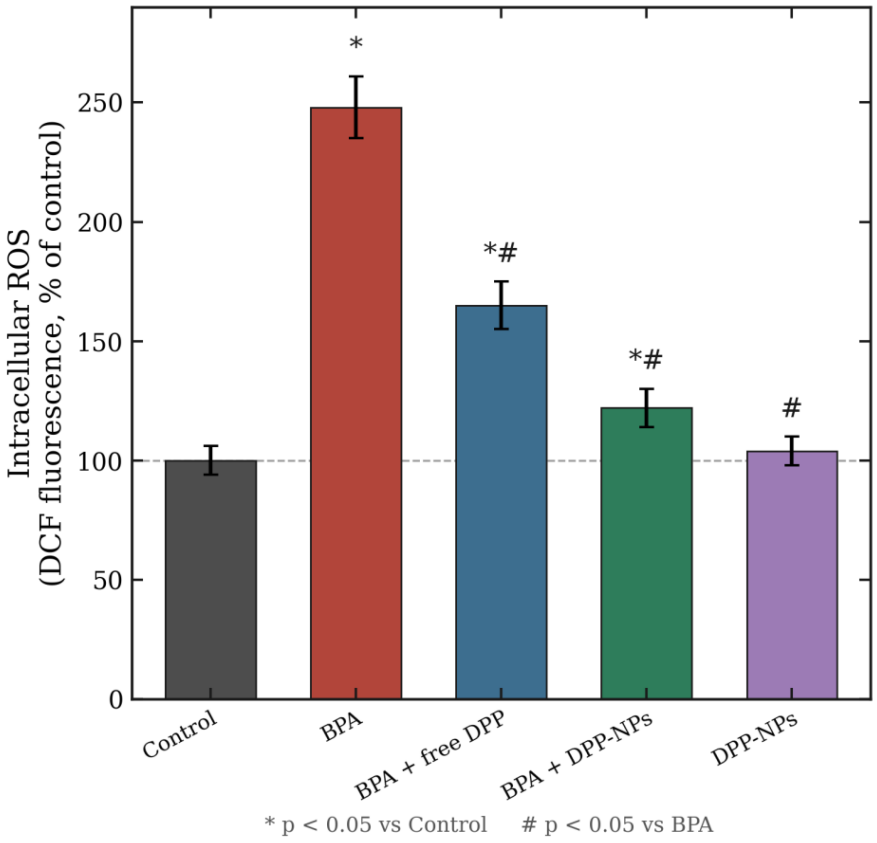

Fig. 4. Intracellular ROS levels (DCFH-DA) in HepG2 cells across the treatment groups: control, BPA alone, BPA + free extract, BPA + loaded nanoparticles, and loaded nanoparticles alone.

Cytotoxicity and selection of the BPA challenge

Before the protection experiments we checked that neither the carrier nor the extract was itself harmful at the doses to be used. The MTT data (Fig. 3) showed that blank nanoparticles were essentially non-toxic across the whole range examined, with viability staying above about 90%, which agrees with the well-documented biocompatibility of chitosan [29]. The free and encapsulated extracts were also well tolerated at low and intermediate concentrations; only at the highest doses did viability begin to fall, and a non-cytotoxic concentration safely below that threshold was chosen for both forms. BPA, by contrast, reduced HepG2 viability in a clear dose-dependent fashion. A sub-lethal concentration that brought viability down to roughly 65% of control was selected as the oxidative-stress challenge for the subsequent assays; comparable sub-lethal exposures have been used by others to model hepatic oxidative injury *in vitro* [5,7].

Protection against BPA-induced cytotoxicity and oxidative stress

Challenging the cells with BPA alone produced the expected picture of oxidative damage. Viability

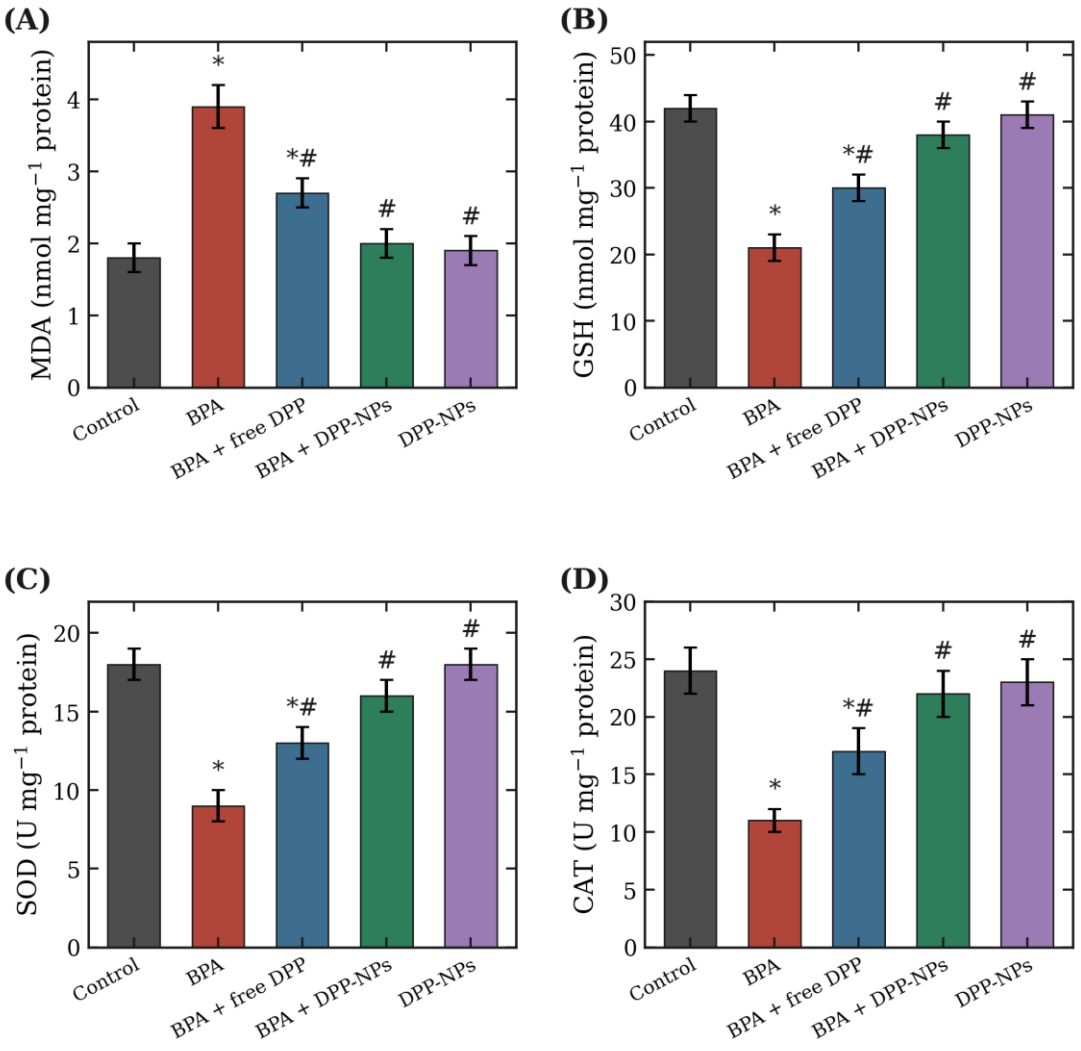

Fig. 5. Lipid peroxidation (MDA) and antioxidant defences (GSH, SOD and CAT) in HepG2 cells across the treatment groups.

dropped to about 65% of control, intracellular ROS rose sharply—to roughly two-and-a-half times the control level—MDA approximately doubled, and the antioxidant defences were eroded, with GSH falling by close to half and the activities of SOD and CAT significantly depressed. Taken together, these shifts describe a state in which BPA-driven radical production has overwhelmed the cell's capacity to detoxify it, and they reproduce, in HepG2 cells, what has repeatedly been seen in BPA-exposed liver tissue and in other cell types [3,4,5,30].

Pre-treatment with the DPP extract counteracted this damage and—importantly—the nano-encapsulated form did so consistently better than the free extract at the same nominal dose. The encapsulated extract restored viability to roughly 88–90% of control, against about 78% for the free extract, and it brought intracellular ROS back close to baseline, whereas the free extract gave only a partial reduction (Fig. 4). The same hierarchy held for the remaining markers: MDA was lowered almost to control values by the nanoparticles but only partly by the free extract, and GSH, SOD and CAT were restored substantially more by the encapsulated form (Fig. 5; Table 3). Cells treated with the loaded nanoparticles alone were indistinguishable from the untreated control, which confirms that the protection was not an artefact of carrier toxicity.

Two complementary explanations can be offered for the superiority of the nanoform. First, encapsulation shields the labile phenolics from oxidation and premature degradation in the culture medium, so that more intact antioxidant reaches the cell; the burst-then-sustained release pattern (Fig. 2) would also keep the intracellular concentration of active compound higher for longer. Second, nanoscale chitosan particles are taken up by cells more readily than free solutes, partly because their positive surface charge favours interaction with the negatively charged cell membrane, which can translate into greater intracellular delivery of the payload [14,28,29]. The net effect is that the same dose of polyphenol simply does more work when it is delivered in nanoparticulate form. Mechanistically, the parallel restoration of GSH and of SOD and CAT activity suggests that the extract supports the enzymatic and non-enzymatic arms of the antioxidant system at once, most likely through direct radical scavenging by its phenolic acids and flavonoids together with the sparing of endogenous antioxidants that follows once the ROS burden falls [9,12]. This is consistent with earlier reports that date-palm and other polyphenol-rich extracts protect the liver against chemically induced oxidative stress [11,12], and with the broader literature showing that flavonoids such as quercetin blunt BPA toxicity through exactly this mix of scavenging and antioxidant-enzyme support [8].

Set against previous nano-encapsulation studies, our results fit a now-familiar theme: encapsulating a plant phenolic in chitosan tends to preserve, and at times amplify, its antioxidant performance relative to the free compound [20,28]. What the present work adds is evidence that this advantage carries through to a functional, cell-based protection endpoint against a relevant environmental toxicant, and that an inexpensive, under-used material—date palm pollen—can serve as the active core. Notably, an alginate-

Table 3. Cell viability, intracellular ROS, malondialdehyde, reduced glutathione, superoxide dismutase and catalase in HepG2 cells across the experimental groups.

Group	Viability (%)	ROS (% control)	MDA (nmol/mg)	GSH (nmol/mg)	SOD (U/mg)	CAT (U/mg)
Control	100 ± 3	100 ± 5	1.8 ± 0.2	42 ± 2	18 ± 1	24 ± 2
BPA (50 µM)	65 ± 4	248 ± 13	3.9 ± 0.3	21 ± 2	9 ± 1	11 ± 1
BPA + free DPP	78 ± 3	165 ± 10	2.7 ± 0.2	30 ± 2	13 ± 1	17 ± 2
BPA + DPP-NPs	89 ± 3	122 ± 8	2.0 ± 0.2	38 ± 2	16 ± 1	22 ± 2
DPP-NPs alone	98 ± 2	104 ± 6	1.9 ± 0.2	41 ± 2	18 ± 1	23 ± 2

Data are mean ± SD ($n \geq 3$); groups were compared by one-way ANOVA with Tukey's post-hoc test ($p < 0.05$). For every parameter the BPA group differed from the control, and both extract-treated groups (BPA + free DPP and BPA + DPP-NPs) differed from the BPA group. The free-extract group remained significantly different from the control for all parameters, whereas the nanoparticle group (BPA + DPP-NPs) returned to control level for MDA, GSH, SOD and CAT and differed from the control only for ROS; the nanoparticles-alone group did not differ from the control for any parameter. Significance markers (*, vs control; #, vs BPA) are shown in Figures 4 and 5.

bead formulation of the same pollen extract was recently shown to protect rat liver against BPA in vivo [17]; the present work complements that study by demonstrating, in a defined HepG2 model, that a chitosan–TPP nanocarrier confers cytoprotection at the cellular level and consistently outperforms the free extract at an equal polyphenol dose. A quantitative comparison of all measured parameters across the treatment groups is presented in Table 3.

A few limitations should be acknowledged. The study is confined to a single cell line and to short-term exposure; the BPA concentration used, though sub-lethal and within the range adopted by others, is higher than typical environmental levels; and protection was assessed only over 24 h. The release and uptake mechanisms were inferred rather than tracked directly. None of this undermines the central finding, but it does mark out the obvious next steps confirmation in primary hepatocytes and in animal models, proper dose–response and longer-term work, and a closer look at the signalling pathways (Nrf2/Keap1 in particular) that are likely to sit downstream of the redox changes observed here [31].

CONCLUSION

A phenolic-rich extract of date palm pollen was successfully entrapped in chitosan–tripolyphosphate nanoparticles by a simple ionic-gelation route. The resulting particles were small, positively charged and reasonably uniform, and the combined FTIR, XRD and FESEM evidence pointed to physical encapsulation of the polyphenols within an amorphous, near-spherical matrix, with an encapsulation efficiency of about 68%. In HepG2 cells, bisphenol A produced a clear oxidative insult—falling viability, elevated ROS and malondialdehyde, and depleted glutathione, superoxide dismutase and catalase. The nano-encapsulated extract reversed these changes more effectively than the free extract given at the same dose, restoring redox balance and antioxidant-enzyme activity while showing no toxicity of its own. Taken together, the data indicate that chitosan-based nano-encapsulation is an effective way to unlock the cytoprotective potential of date palm pollen polyphenols, and that the nanoformulation deserves further evaluation as a low-cost agent against bisphenol A-related hepatic oxidative damage. Follow-up studies in primary cells and animal models, with attention to dose and to the underlying signalling, are the logical continuation of this work.

CONFLICT OF INTEREST

The authors declare that there is no conflict of interests regarding the publication of this manuscript.

REFERENCES

1. Vandenberg LN, Hauser R, Marcus M, Olea N, Welshons WV. Human exposure to bisphenol A (BPA). Reprod Toxicol. 2007;24(2):139-177.
2. Rochester JR. Bisphenol A and human health: A review of the literature. Reprod Toxicol. 2013;42:132-155.
3. Hassan ZK, Elobeid MA, Virk P, Omer SA, ElAmin M, Daghestani MH, et al. Bisphenol A Induces Hepatotoxicity through Oxidative Stress in Rat Model. Oxid Med Cell Longev. 2012;2012:1-6.
4. Khan S, Beigh S, Chaudhari BP, Sharma S, Aliul Hasan Abdi S, Ahmad S, et al. Mitochondrial dysfunction induced by Bisphenol A is a factor of its hepatotoxicity in rats. Environ Toxicol. 2015;31(12):1922-1934.
5. Huc L, Lemarié A, Guéraud F, Héliès-Toussaint C. Low concentrations of bisphenol A induce lipid accumulation mediated by the production of reactive oxygen species in the mitochondria of HepG2 cells. Toxicol In Vitro. 2012;26(5):709-717.
6. Moon MK, Kim MJ, Jung IK, Koo YD, Ann HY, Lee KJ, et al. Bisphenol A Impairs Mitochondrial Function in the Liver at Doses below the No Observed Adverse Effect Level. J Korean Med Sci. 2012;27(6):644.
7. Ooe H, Taira T, Iguchi-Ariga SMM, Ariga H. Induction of Reactive Oxygen Species by Bisphenol A and Abrogation of Bisphenol A-Induced Cell Injury by DJ-1. Toxicol Sci. 2005;88(1):114-126.
8. Shirani M, Alizadeh S, Mahdavinia M, Dehghani MA. The ameliorative effect of quercetin on bisphenol A-induced toxicity in mitochondria isolated from rats. Environmental Science and Pollution Research. 2019;26(8):7688-7696.
9. Valko M, Leibfritz D, Moncol J, Cronin MTD, Mazur M, Telser J. Free radicals and antioxidants in normal physiological functions and human disease. The International Journal of Biochemistry and Cell Biology. 2007;39(1):44-84.
10. Habib HM, El-Fakharany EM, El-Gendi H, El-Ziney MG, El-Yazbi AF, Ibrahim WH. Palm Fruit (Phoenix dactylifera L.) Pollen Extract Inhibits Cancer Cell and Enzyme Activities and DNA and Protein Damage. Nutrients. 2023;15(11):2614.
11. Saafi EB, Louedi M, Elfeki A, Zakhama A, Najjar MF, Hammami M, et al. Protective effect of date palm fruit extract (Phoenix dactylifera L.) on dimethoate induced-oxidative stress in rat liver. Experimental and Toxicologic Pathology. 2011;63(5):433-441.
12. Vayalil PK. Date Fruits (Phoenix dactylifera Linn): An Emerging Medicinal Food. Critical Reviews in Food Science and Nutrition. 2012;52(3):249-271.
13. Fang Z, Bhandari B. Encapsulation of polyphenols – a review. Trends in Food Science and Technology. 2010;21(10):510-523.
14. Liang J, Yan H, Puligundla P, Gao X, Zhou Y, Wan X. Applications of chitosan nanoparticles to enhance absorption and bioavailability of tea polyphenols: A review.

Food Hydrocolloids. 2017;69:286-292.
15. Belščak-Cvitanović A, Stojanović R, Manojlović V, Komes D, Cindrić IJ, Nedović V, et al. Encapsulation of polyphenolic antioxidants from medicinal plant extracts in alginate–chitosan system enhanced with ascorbic acid by electrostatic extrusion. Food Res Int. 2011;44(4):1094-1101.
16. Calvo P, Remu□□n-L□pez C, Vila-Jato JL, Alonso MJ. Novel hydrophilic chitosan-polyethylene oxide nanoparticles as protein carriers. J Appl Polym Sci. 1997;63(1):125-132.
17. Fouda K, Mohamed RS. Alginate Beads with Encapsulated Date Palm Pollen Extract: Development, Characterization and Their Potential Role in Hepato-Protection and Fertility-Stimulating Hormones Improvement in Bisphenol A-Treated Rats. Polymers. 2025;17(7):912.
18. Singleton VL, Rossi JA. Colorimetry of Total Phenolics with Phosphomolybdic-Phosphotungstic Acid Reagents. American Journal of Enology and Viticulture. 1965;16(3):144-158.
19. Brand-Williams W, Cuvelier ME, Berset C. Use of a free radical method to evaluate antioxidant activity. LWT - Food Science and Technology. 1995;28(1):25-30.
20. Soleymanfallah S, Khoshkhoo Z, Hosseini SE, Azizi MH. Preparation, physical properties, and evaluation of antioxidant capacity of aqueous grape extract loaded in chitosan-TPP nanoparticles. Food Science and Nutrition. 2022;10(10):3272-3281.
21. Mosmann T. Rapid colorimetric assay for cellular growth and survival: Application to proliferation and cytotoxicity assays. J Immunol Methods. 1983;65(1-2):55-63.
22. Wang H, Joseph JA. Quantifying cellular oxidative stress by dichlorofluorescein assay using microplate reader11Mention of a trade name, proprietary product, or specific equipment does not constitute a guarantee by the United States Department of Agriculture and does not imply its approval to the exclusion of other products that may be suitable. Free Radical Biology and Medicine. 1999;27(5-6):612-616.
23. Ohkawa H, Ohishi N, Yagi K. Assay for lipid peroxides in animal tissues by thiobarbituric acid reaction. Anal Biochem. 1979;95(2):351-358.
24. Ellman GL. Tissue sulfhydryl groups. Archives of Biochemistry and Biophysics. 1959;82(1):70-77.
25. Marklund S, Marklund G. Involvement of the Superoxide Anion Radical in the Autoxidation of Pyrogallol and a Convenient Assay for Superoxide Dismutase. Eur J Biochem. 1974;47(3):469-474.
26. Aebi H. [13] Catalase in vitro. Methods in Enzymology: Elsevier; 1984. p. 121-126. http://dx.doi.org/10.1016/s0076-6879(84)05016-3
27. Al-Farsi* MA, Lee CY. Nutritional and Functional Properties of Dates: A Review. Critical Reviews in Food Science and Nutrition. 2008;48(10):877-887.
28. Wang W, Jung J, Zhao Y. Chitosan-cellulose nanocrystal microencapsulation to improve encapsulation efficiency and stability of entrapped fruit anthocyanins. Carbohydr Polym. 2017;157:1246-1253.
29. Bhattarai N, Gunn J, Zhang M. Chitosan-based hydrogels for controlled, localized drug delivery. Adv Drug Del Rev. 2010;62(1):83-99.
30. Nakagawa Y, Tayama S. Metabolism and cytotoxicity of bisphenol A and other bisphenols in isolated rat hepatocytes. Arch Toxicol. 2000;74(2):99-105.
31. Ma H, Wang H, Chen H, Hou H, Hu Q. Nicotine-quercetin combination alleviate ulcerative colitis via PI3K/AKT and NF-κB pathway inhibition. Chin Sci Bull. 2025;71(10):2283-2298.